

Comparison of Different Pitch Controller In Wind Farm For Integrated Power System

Md. Shizer Rahman¹, Md. Shoaib Akther² & Md. Habib Ehsanul Hoque³

¹Lecturer, Department of Electrical & Electronic Engineering, Pundra University of Science & Technology, Gokul, Bogra-5800, Bangladesh.

²Lecturer, Department of Electrical & Electronic Engineering, Bangladesh Army University of Science and Technology (BAUST), Saidpur cantonment, Saidpur-5310, Bangladesh.

³Lecturer, Department of Computer Science & Engineering, Pundra University of Science & Technology, Gokul, Bogra-5800, Bangladesh.

Corresponding author: Md. Shizer Rahman

ABSTRACT: The speed of wind is not constant as well as the generated voltage is not also constant. In some cases, the strong typhoons destroy the stand-alone turbines. Second, sometimes the wind speeds are very low and not enough to produce electricity. Third, if there's enough wind, wind speeds are not constant at all times, thus creating fluctuations in electricity that damage the load. For this reason pitch angle control is the most common means for adjusting the aerodynamic torque of the wind turbine when wind speed is above or below rated speed. As conventional pitch control usually use PI controller, where the mathematical model of the system should be known well. The comparisons with conventional pitch angle control strategies with various controlling variables will be carried out.

KEYWORDS - Wind power, Blade Pitch Angle Control (BPA), Wind Energy Conversion System (WECS), wind turbine generation systems (WTGS).

Date of Submission: 15-03-2018

Date of acceptance: 30-03-2018

I. INTRODUCTION

Recently, shortages of fossil fuel and environmental global warming have become serious problems. It is thus necessary to introduce clean energy more in place of the fossil fuel. As wind power is one of the prospective clean energy resources, a large number of wind farms are being in service in the world. Many wind turbine generation systems (WTGS) are being in operation presently in the world. A huge number of new WTGS are going to be connected with the utility network every year. This rapid increase of the number of WTGSs operating in the power systems, on the one hand, introduces problems for the integrated power system. In the other hand, shows the importance and necessity of their operation in power system analysis [1]. One of the simplest methods of operating a WTGS is to use an induction generator (IG) connected directly to the power grid, because an induction generator is the most cost-effective and robust machine for wind energy conversion. However, during startup, the induction generators need reactive power. As the reactive power drained by the induction generators is coupled to the active power generated by them, the variation of wind speed causes the variations of IGs real and reactive powers. These active and reactive power variations interact with the network and thus initiate voltage and power fluctuations. Thus, reactive power compensation is a major issue; especially for fixed-speed WTGS for both steady state and transient conditions. Usually, a capacitor bank is placed at wind farm terminal to provide the necessary reactive power demand at steady state. But it cannot maintain the wind generator terminal voltage constant under the randomly fluctuating wind speed. Moreover, IG needs a large reactive power during short circuit faults. Due to the weakness of shunt capacitor banks in maintaining voltage stability as well as reactive power improvement at point of common coupling and wind turbine generator bus, STATCOM, SVC and FACT as dynamic VAR compensators have been attached at the transmission network to support the stability [2-4]. An automatic power management system to monitor the distribution of power is presented using PI pitch angle control to a set of load banks [5] and optimizing the wind turbine rotor speed set point algorithm is depicted using a Particle Swarm Optimization (PSO)-based wind

turbine speed set point algorithm [6]. The dynamic behavior of a DFIG grid connected, wind energy conversion system (WECS) is simulated using MATLAB under different fault condition [7]. Artificial Neural Network (ANN) control technique has been developed for Doubly Fed Induction Generator (DFIG) based wind energy generation system [8]. DQ-axis control and a distributed (independent) control for both individual pitch and trailing edge flap smart rotor control discussed for load reduction [5]. The output frequency of a wind turbine system supplying an isolated load is regulated by controlling the rotor speed of the turbine using a PID controller [9]. Elimination of harmonics using wind energy conversion Systems introduced to reduce the distortion of the voltage waveforms i.e. harmonics may cause overheating of neutral conductors and electrical distribution transformers, the malfunction of electronic equipment and the distortion of communication systems [10]. The comparison of variable speed wind turbine (VSWT) and fixe speed wind turbine (FSWT has been analysis to model the WTGS [11-12].

II. WIND SPEED AND POWER CHARECTERISTIC

2.1 Wind Steam power

The kinetic energy in air of an object of mass M moving with speed V is represented by the following equation:

$$E = \frac{1}{2}MV^2 \dots\dots\dots (1)$$

The power in the moving air (assuming constant wind velocity) is equal to:

$$P_{wind} = \frac{dE}{dt} = \frac{1}{2}MV^2 \dots\dots\dots (2)$$

Where, M is the mass flow rate per second. When the air passes across the swept area A, the power in the air can be computed as

$$P_{wind} = \frac{1}{2}(\rho VA)V^2 = \frac{1}{2}\rho AV^3 \dots\dots\dots (3)$$

Where, ρ is the air density. Air density varies with air pressure and temperature in accordance with the gas law:

$$\rho = \frac{p}{RT} \dots\dots\dots (4)$$

Where, p = Air pressure, T = Temperature, R = Gas constant. The pressure and temperature also varies with the wind turbine location. In the case of propeller type turbine, if the diameter of the rotating blades is d then the swept area

$$A = \pi\left(\frac{d}{2}\right)^2, \text{ and substituting it in equation (3), the wind power become, } P_{wind} = \frac{1}{8}\pi\rho d^2V^3$$

2.2 Power Output from Practical Wind Turbines

The function of power extracted from the power in the wind by a practical wind turbine is usually given by the symbol C_p , standing for the co-efficient of performance or power co-efficient [13, 14]. Using this notation and dropping the subscripts of eq. (5), the actual mechanical power output can be written as,

$$P_m = C_p \frac{1}{2}(\rho AV_w^3) = \frac{1}{2}\rho\pi R^2 V_w^3 C_p(\lambda, \beta) \dots\dots\dots (5)$$

Where,

R is the blade radius of the wind turbine[m],

V_w is the wind speed [m/sec],

ρ is the air density[kg/m³].

The co-efficient of performance is not constant, varies with the wind speed, the rotational speed of the turbine, and the turbine blade parameters like angle of attack and pitch angle. Generally, it is said that power co-efficient, C_p is the function of the tip speed ratio, λ , and blade pitch angle, [degree].

$$\lambda = \frac{\omega_R R}{V_w}$$

Where,

ω_R is the mechanical angular velocity of the turbine rotor in rad/s and

V_w is the wind speed in m/s.

The angular velocity, ω_R is determined from the rotational speed, n(r/min) by the equation

$$\omega_R = \frac{2\pi n}{60}$$

A generic equation is used to model $C_p(\lambda, \beta)$. This equation, based on the modeling turbine characteristics, is:

$$C_p(\beta, \lambda) = C_1\left(\frac{C_2}{\lambda_i} - C_3\beta - C_4\right) e^{-\frac{C_6}{\lambda_i}} + C_6\lambda \dots\dots\dots (6)$$

$$\frac{1}{\lambda_i} = \frac{1}{\lambda + 0.08\beta} - \frac{0.035}{\beta^3 + 1} \dots\dots\dots (7)$$

Where the coefficients C_1 to C_6 are: $C_1 = 0.5176$, $C_2 = 116$, $C_3 = 0.4$, $C_4 = 5$, $C_5 = 21$ and $C_6 = 0.0068$.

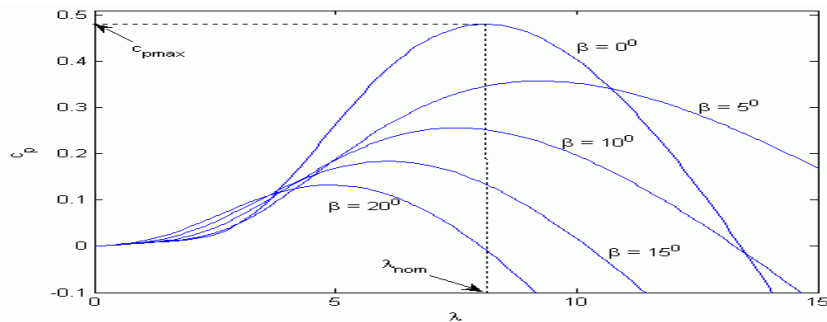


Figure 1: Performance coefficient vs tip speed at different pitch angle

From the C_p - λ characteristics, for different values of the pitch angle β , are illustrated above. The maximum value of C_p ($C_{p\max} = 0.48$) is achieved for $\beta = 0$ degree and for $\lambda = 8.1$. This particular value of λ is defined as the nominal value (λ_{nom}). Performance coefficient vs tip speed at different pitch angle is shown in Fig. 1.

The mechanical power P_m as a function of generator speed, for different wind speeds and for blade pitch angle $\beta = 0$ degree.

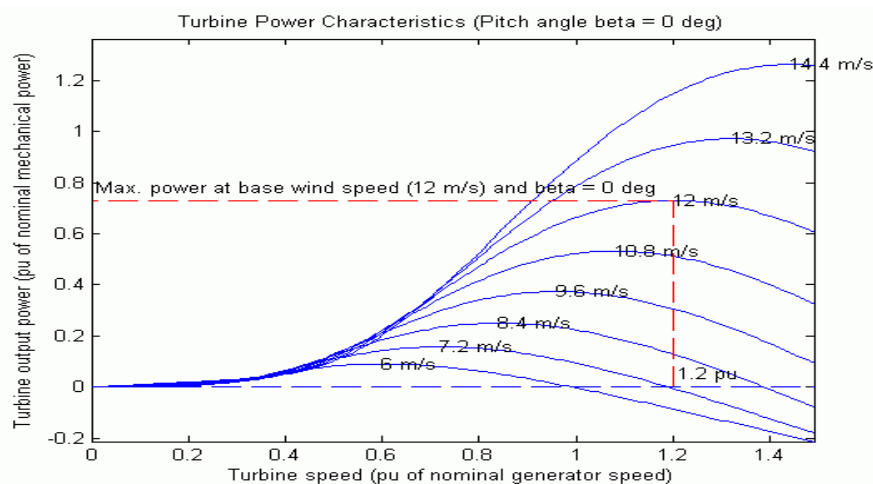


Figure 2: Turbine power characteristics at 0° pitch angle

The C_p is the fraction of the upstream wind power, which is captured by the rotor blades. The remaining power is discharged or wasted in the downstream wind. The factor C_p is called the power coefficient of the rotor or the rotor efficiency. For a given upstream wind speed, the value of C_p depends on the ratio of the downstream to the upstream wind speeds. The plot of power coefficient versus tip speed ratio shows that C_p is a single, maximum-value function. It has the maximum value of 0.59. The maximum power is extracted from the wind at that speed ratio. The theoretical maximum value of C_p is 0.59. In practical designs, the maximum achievable C_p is below 0.5 for high-speed, two-blade turbines, and between 0.2 and 0.4 for slow speed turbines with more blades [15].

III. SYSTEM DESIGN AND SIMULATION

3.1 Model System for Simulation Analysis

The model system shown in Fig.3 has been used for the simulation analyses of wind generator stabilization, in this work. The model system consists of a wind turbine generator (50MVA induction generator, IG), which are delivering power to an infinite bus through a transmission line. Though a wind power station is composed of many generators, it is considered to be composed of a single generator with the total power capacity. There is a local transmission line with one circuit between the main transmission line and the transformer followed by the wind power station. A double squirrel-cage induction machine model Fig. 6, which is represented by the steady state equivalent circuit shown in Fig. 8, where s denotes a rotational slip, is used for the wind generator. To establish the rotating magnetic field of the stator, reactive power is needed to be supplied from the network to the stator winding of the induction generator. Therefore, to compensate the reactive power demand at steady state, a capacitor bank is inserted at the terminal of IG [16-17]. The value of the capacitor (0.2393pu) is chosen in such a way that the power factor of the wind power station becomes unity during the rated condition ($V=1.0$, $P=0.5$) [16-17].

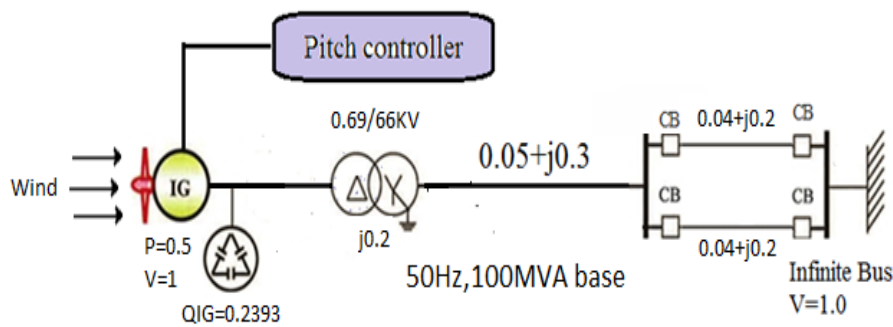


Figure 3: Power system model

3.2 Model System Analysis

The model of wind turbine rotor is complicated. According to the blade element theory [13], modeling of blade and shaft need complicated and lengthy computations. Moreover, it also needs detailed and accurate information about rotor geometry. For that reason, considering only the electrical behavior of the system, a simplified method of modeling of the wind turbine blade and shaft is normally used. In this paper, The MOD-2 characteristic is used for wind turbine model. Modeling expression of MOD-2 is given as follows [15]. The captured power from the wind can be obtained from (8).

$$P_w = 0.5 \rho \pi R^2 V_w^3 C_p(\beta, \lambda) \dots \dots \dots (8)$$

Where P_w , is the extracted power from the wind, ρ is the air density [kg/m^3], R is the blade radius [m] and C_p is the power coefficient which is a function of both tip speed ratio, λ , and blade pitch angle, β [deg]. λ and C_p are expressed as (9) and (10).

$$\lambda = \frac{V_w}{\omega_B} \dots \dots \dots (9)$$

$$C_p = 0.5(\lambda - 0.022\beta^2 - 5.6)e^{-0.17\lambda} \dots \dots \dots (10)$$

where, ω_B is the rotational speed of turbine hub [rad/s]. Here wind speed, V_w , is in mile/hr. When the wind velocity exceeds the rated speed, then the pitch angle of the blade needs to be controlled to maintain the output to control the output power nearly constant at rated capacity [18]. Now the turbine torque, T_w , can be calculated from Eq. (11),

$$T_w = 0.5 \rho \pi R^2 V_w^3 C_p(\beta, \lambda) / \lambda \dots \dots \dots (11)$$

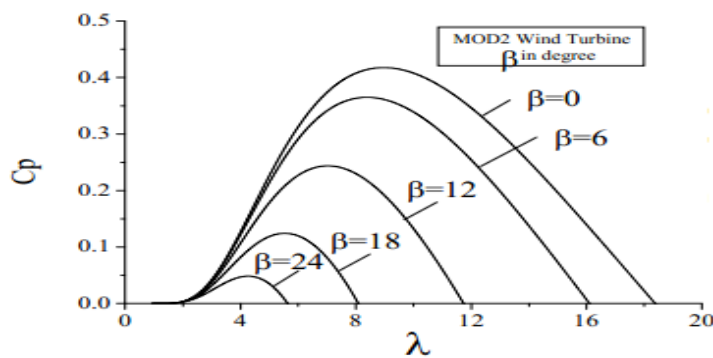


Figure 4: C_p - λ curves for different angles

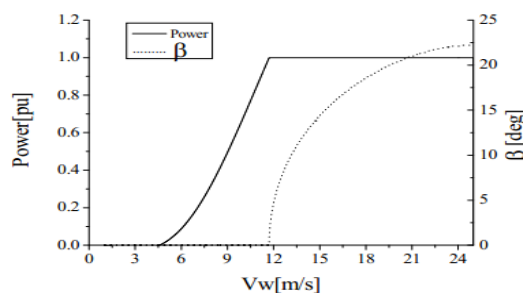


Figure 5: Power vs V_w and pitch angle(β) vs V_w characteristic

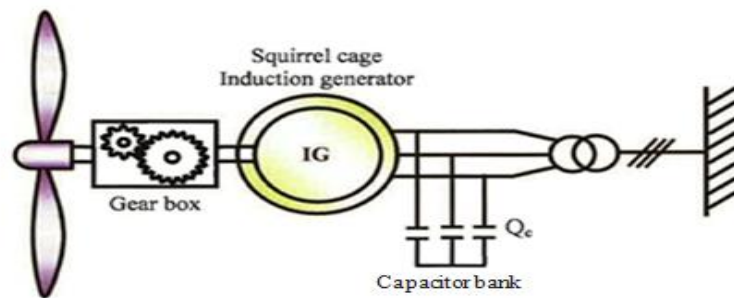


Figure 6: Squirrel case Induction generator

3.3 Equivalent Circuit Analysis

Both single and double cage induction generators are used as fixed-speed wind generators. The equivalent circuits of single and double cage induction generators are shown in Fig. 7 and Fig. 8, respectively, where s denotes rotational slip. From the single cage equivalent circuit of an IG shown in Fig. 7, the loop equations can be derived as Equation 12 and 13. From these two equations we can obtain the desired currents I_1 and I_2 . Again, from the equivalent circuit of a single cage IG,

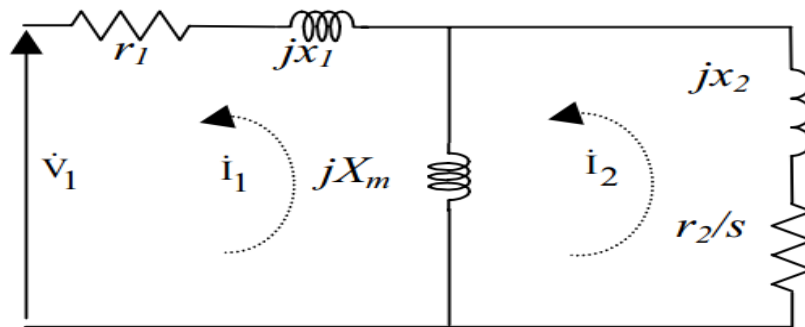


Figure 7: Steady state equivalent circuit of single squirrel-case induction generator

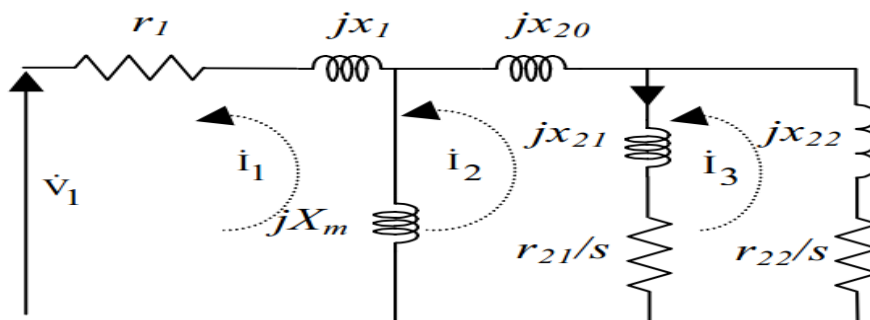


Figure 8: Steady state equivalent circuit of double squirrel-case induction generator

We can calculate the input power of the induction generator, $P_{IG_IN_SINGLE}$, which is actually the output power of the wind turbine, shown in Eq. 9. From doublecage equivalent circuit of the induction generator shown in Fig. 8, the loop equations can be derived as Equations 15 and 16. From these three equations we can get the desired currents I_1 , I_2 , and I_3 . From the equivalent circuit of the double cage induction generator, we can calculate the input power of induction generator, $P_{IG_IN_DOUBLE}$, shown in Eq. 17. We can also calculate the desired output power of both single and double cage induction generators, P_{IG_OUT} , shown in Eq. 18, from the equivalent circuits shown in Figs.7 and 8.. The detailed description of the WTGS subroutine is presented below, in the light of the single cage equivalent circuit of the induction generator

$$V_1 = -(r_1 + jx_1 + jx_m)I_1 + jx_m I_2 \dots \dots \dots (12)$$

$$0 = jx_m I_1 - (\frac{r_2}{s} + jx_2 + jx_m)I_2 \dots \dots \dots (13)$$

$$P_{IG_IN_SINGLE} = I_2^2 \frac{(1-s)}{s} r_2 \dots \dots \dots (14)$$

$$0 = jx_m I_1 - (\frac{r_{21}}{s} + jx_{21} + jx_{20} + jx_m)I_2 + (\frac{r_{21}}{s} + jx_{21})I_3 \dots \dots \dots (15)$$

$$0 = \left(\frac{r_{21}}{s} + jx_{21}\right)I_2 - \left(\frac{r_{21}}{s} + \frac{r_{22}}{s} + jx_{21} + jx_{22}\right)I_3 \dots\dots\dots (16)$$

$$P_{IG_IN_DOUBLE} = I_3^2 \frac{(1-s)}{s} r_{22} + (I_3 - I_2)^2 \frac{(1-s)}{s} r_{21} \dots\dots\dots (17)$$

$$P_{IG_OUT} = Re[V_1 I_1^*] \dots\dots\dots (18)$$

3.4 Pitch Controller

When the wind speed exceeds the rated speed, the pitch angle needs to be controlled. In this paper, the conventional pitch controller shown in Fig. 9 is used. The purpose of using the pitch controller is to maintain the output power of the wind generator at rated level by controlling the blade pitch angle of turbine blade when the wind speed is over the rated speed [16]. In some studies, this pitch controller is used to enhance the transient stability of WTGS when network disturbance occurs in the power system. The pitch servo is modeled with a first order delay system with a time constant $T_d=5$ sec. Because of the mechanical constraint, the pitch actuation system cannot, in general, respond instantly, and thus a rate limiter with a value of $10^0/\text{sec}$ is added to obtain the realistic response [18]. PI controller is used in the control system block. The value of proportional gain and integral time constant are chosen as 60 and 0.03, respectively.

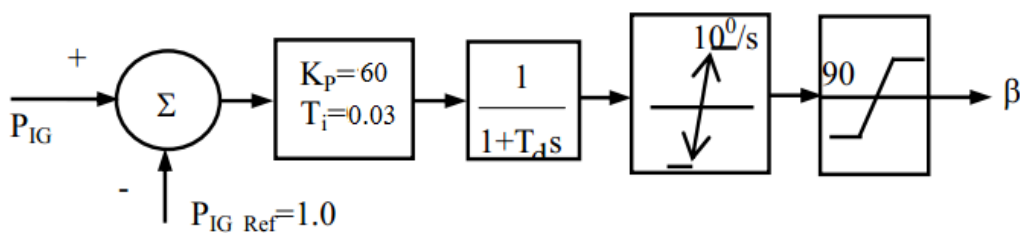


Figure 9: Pitch angle control

3.5 Generation of Line Power Reference Using Low Pass Filter (LPF)

Reference value of the transmission line power, is determined by using a low pass filter (LPF) as shown in Fig. 10. The LPF suggests an increase or a decrease in the level of wind power output, which corresponds to charging or discharging of the stored energy.

Though it is very simple, it can be understood from Fig. 11 that reference value with enough smoothing effect can be obtained by using this type of LPF. Fig. 11 shows an example how the time constant, T, affects the filtered wind power in practice. The values of T in the Fig. 11 correspond to energy storages system with different energy capacities. It is seen that the wind power fluctuation decreases as the LPF time constant increases. Therefore, if the transmission line power is compensated according to the reference value, P_{line_ref} it is possible to decrease the system frequency fluctuation due to the wind generator output fluctuations.

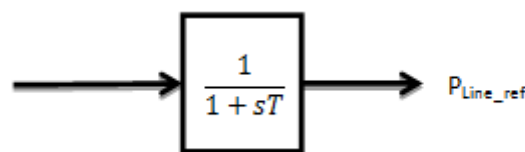


Figure 10: Determination of reference line power

The first-order passive low pass filter can be mathematically described as,

$$P_{IG} = P_{Lref} + T * P'_{Lre} \dots\dots\dots (19)$$

where T is the filtering time constant corresponding to energy storage capacity, P_{Lref} is the filter output function corresponding to the wind turbine output together with the storage unit, P'_{Lref} is the derivative of P and P_{IG} is the filter input function that corresponds to the wind turbine output without energy storage. When discrete data with a time step are applied to a low pass filter and the derivative of P_{Lref} is expanded into a discrete form, equation (19) can be written for step k as,

$$P_{Lref,k} = \frac{T}{T+\Delta t} P_{Lref,k-1} + \frac{\Delta t}{T+\Delta t} P_{IG,K} \dots\dots\dots (20)$$

Defining a constant, $\beta = \frac{T}{T+\Delta t}$, equation (20) can be rewritten as,

$$P_{Lref,k} = \beta P_{Lref,k-1} + (1-\beta) P_{IG,k} \dots\dots\dots (21)$$

Now equation (21) has the form of an exponential weighted moving average (EWMA) filter[14]. The subscript k corresponds to time, i.e. $t_k = t_0 + k\Delta t$, where Δt is the time step and t_0 is the starting point of the analysis. With a EWMA filter the response of the energy storage system is

$$P_{st,k} = P_{IG,k} - P_{Lref,k} \dots\dots\dots (22)$$

Where $P_{st,k}$ is the power absorbed by the storage unit. Thus, the level of the stored energy on the system is in discrete form as

$$E_k = \sum_{m=1}^k P_{st,m} \Delta t \dots\dots\dots (23)$$

The energy storage capacity used for damping the fluctuations is then defined as

$$E_{storage} = \text{Max}E_k - \text{Min}E_k, \text{ for } k=1 \dots\dots n, \dots\dots\dots (24)$$

Where n is the total number of time positions in the data sample.

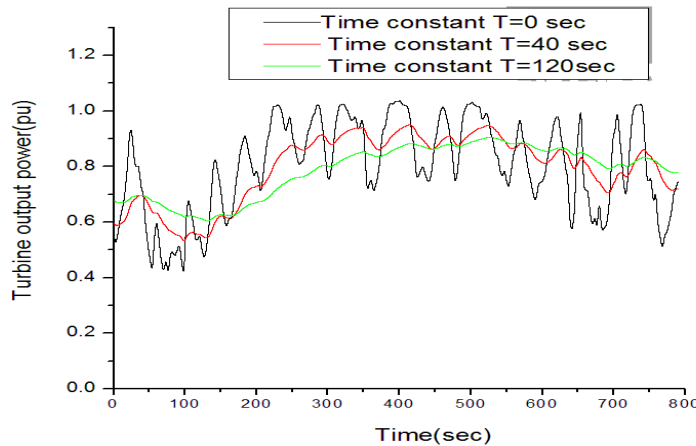


Figure 11: Effect of Time constant on the filtered wind power

3.6 Generation of Line PowerReference Using Simple Moving Average (SMA)

The n period SMA [16] for period d is computed by,

$$SMA_d = \frac{\sum_{i=1}^n M_{(d-i)+1}}{n}; (n \leq d) \dots\dots\dots (25)$$

If ten measurements, M_1 through M_{10} are available, these successive 4 period simple moving average, for example, are as follows:

$$SMA_4 = (M_4 + M_3 + M_2 + M_1) / 4 \dots\dots\dots (26)$$

$$SMA_5 = (M_5 + M_4 + M_3 + M_2) / 4 \dots\dots\dots (27)$$

.
.

.

.

.

$$SMA_{10} = (M_{10} + M_9 + M_8 + M_7) / 4 \dots\dots\dots (28)$$

It is not possible to compute a 4 period moving average until 4 periods data are available. That's why the first moving average in the above example is SMA_4 . [13, 19]

3.6 Generation of Line PowerReference Using Exponential Moving Average (EMA)

The N periods EMA [9] is calculated using the formula shown below:

$$EMA(C) = [(C-P) * K] + P \dots\dots\dots (29)$$

Where C= current value, P= previous period's EMA and K= weighting factor. For a period-based EMA, "K" is equal to $2 / (1 + N)$, where N is the specified number of periods. For example, a 10- period EMA's "weighting factor" is calculated like this: $2/(1+10)=0.1818$. [13, 19]

IV. SIMULATION RESULTS

The simulations have been done by using PSCAD/EMTDC [20]. The time step and simulation time have been chosen as 0.00001 sec and 800 sec respectively. In this simulation, the wind speed used in the model system of Fig. 3 is shown in Fig. 12 here wind speed is varies from 8.5m/s to 13.5m/s. The conventional pitch controller shown in Fig. 9 is used to control the ig output power at rated level when the wind speed is above the rated speed. Fig. 13 shows the real power of ig with using only the conventional pitch controller. The conventional pitch controller works only when wind speed is over the rated speed. Fig. 15 shows the reactive power of ig. The wind turbine blade pitch angle response is also shown in Fig. 15 and Fig. 16 shows the terminal voltage responses of ig. it is seen that the conventional pitch controller cannot smooth well the wind generator output power and terminal voltage. The grid connected real and reactive power is shown in Fig. 17 and fig. 18 respectively. Grid filtered power and grid line voltage is also shown in Fig. 19 and Fig. 20 respectively. The reference line power is calculated by using SMA [as shown in Fig. 21], EMA [as shown in Fig. 22] and LPFSMA [as shown in Fig. 23]. From Fig. 24 shows the comparison with SMA, EMA and LPF. As

wind is fluctuating in nature, the output power and terminal voltage of wind generator also fluctuate randomly. The proposed technique can smooth the wind farm output power according to the reference line power. From the above comparison it can be said that, the LPF method is better for reference line power generation.

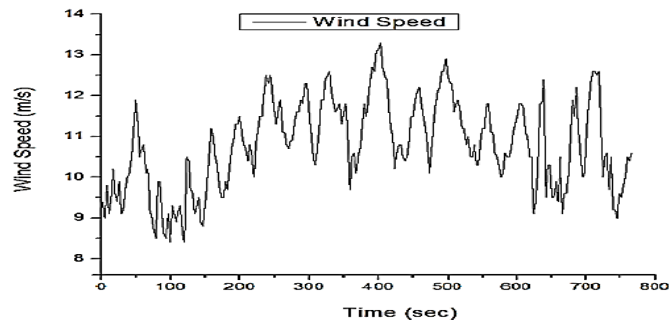


Figure 12: Wind speed using in wind turbine

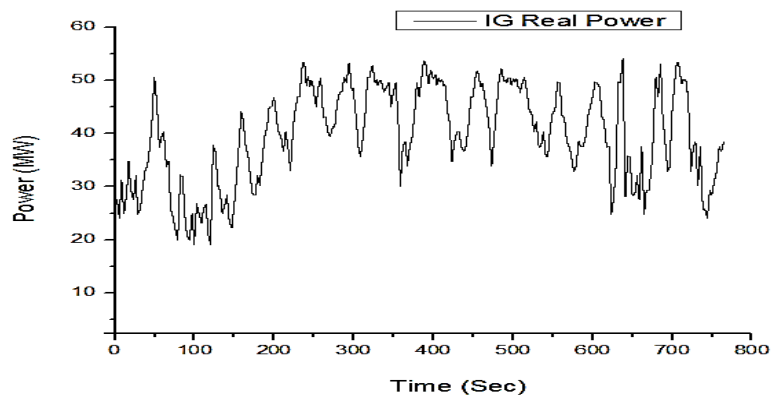


Figure 13: Real power of Induction Generator (IG)

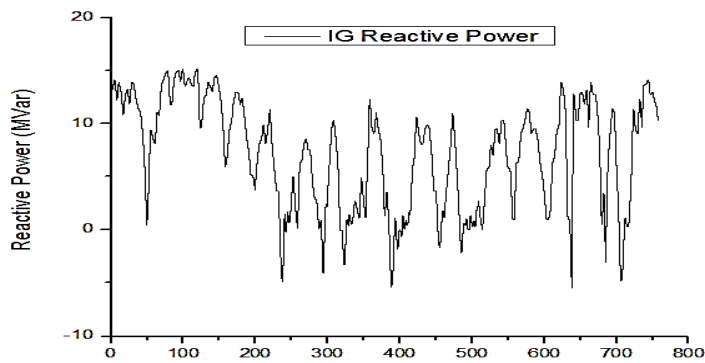


Figure 14: Reactive power of Induction Generator (IG)

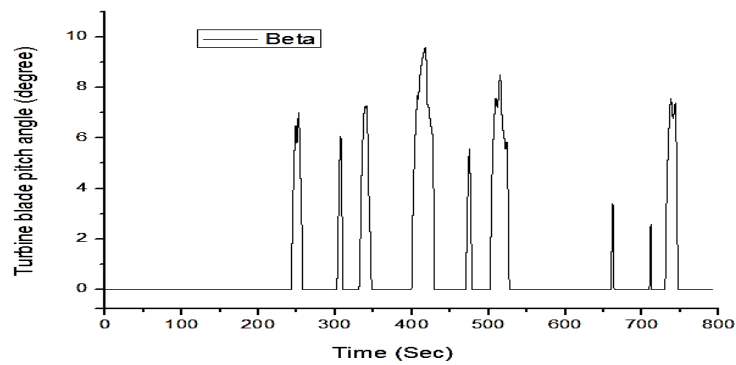


Figure 15: Response of blade pitch angle of wind turbine

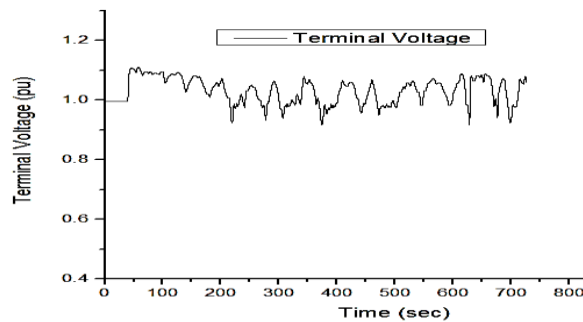


Figure 16: Terminal voltage of Induction Generator (IG)

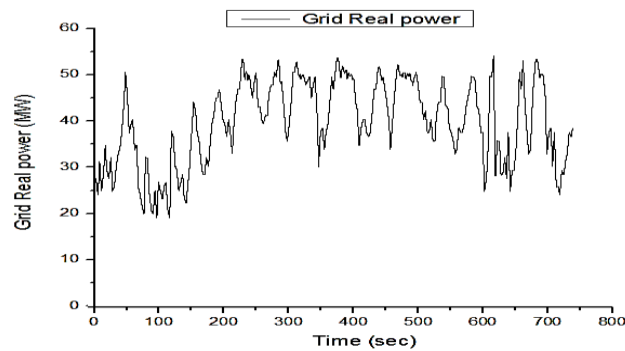


Figure 17: Grid Real Power

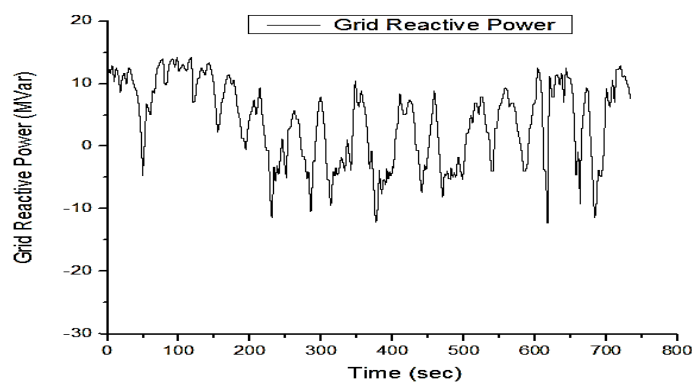


Figure 18: Grid Reactive Power

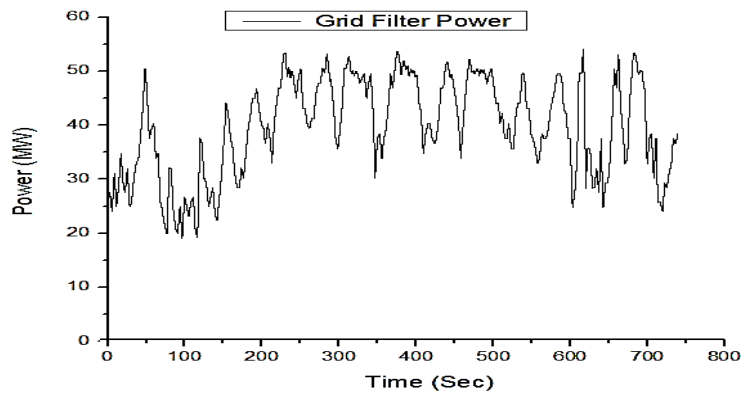


Figure 19: Grid Filtered Power

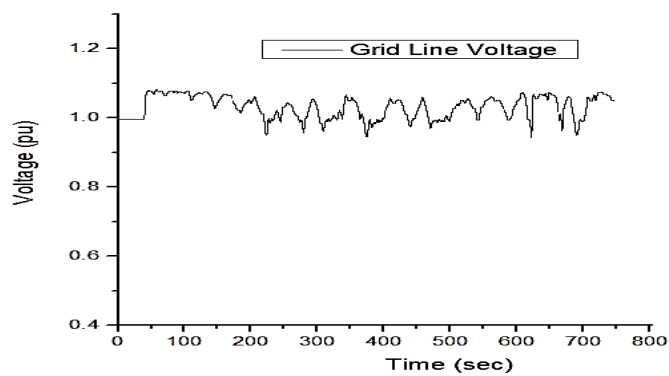


Figure 20: Grid Line voltage

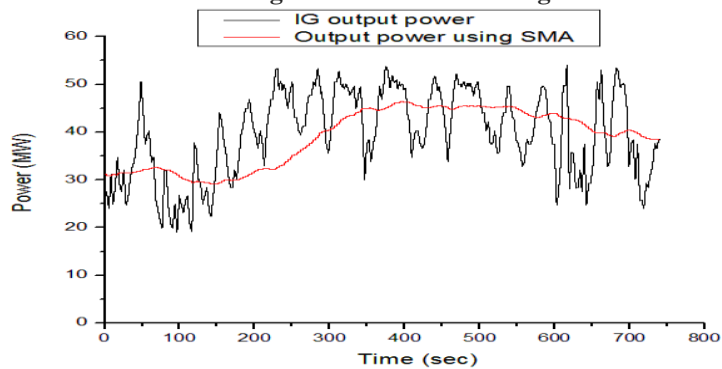


Figure 21: Wind Farm Output Power Using SMA

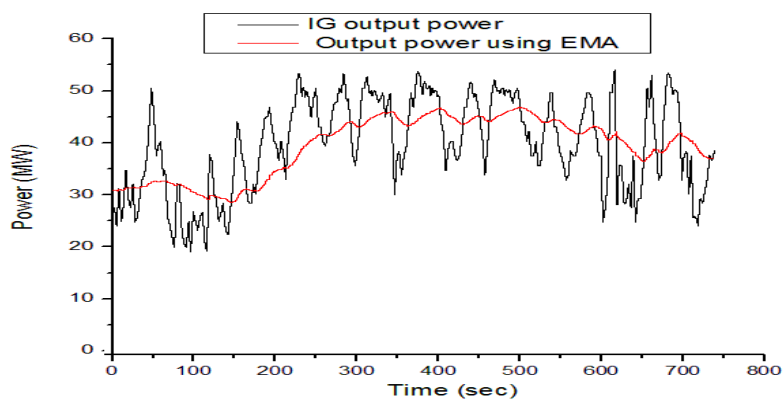


Figure 22: Wind Farm Output Power Using EMA

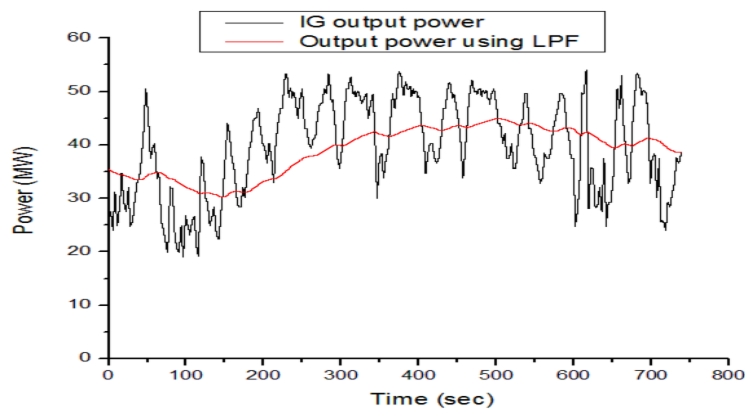


Figure 23: Wind Farm Output Power Using LPF

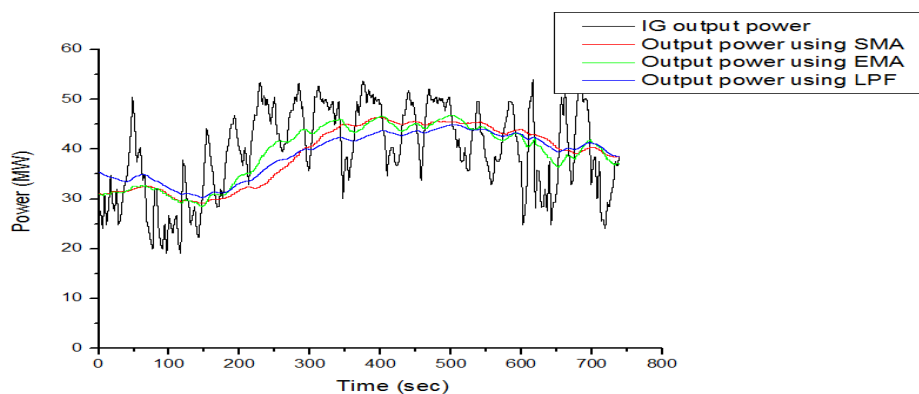


Figure 24: Wind Farm Output Power Using SMA, EMA & LPF

V. CONCLUSION

As wind is fluctuating in nature, the output power and terminal voltage of wind generator also fluctuate randomly. The Pitch angle control is the most common means to control the aerodynamic power generated by the wind turbine rotor. Pitch angle control also has an effect on the aerodynamic loads which may be controlled by the controller to achieve lower torque peak as well as lower fatigue loads. The conventional pitch angle control strategy using different controlling variables can be implemented. However, from the simulation results it can be conclude that PI controller pitch angle control strategy is the most effective method then conventional pitch controller.

REFERENCES

- [1]. Local Government Engineering Department (LGED), "Sustainable Rural Energy" web site(<http://www.lged.org/sre>).
- [2]. Qusay Salem and Ibrahim Altawil, Stability Study of Grid Connected to Multiple Speed Wind Farms with and without FACTS Integration, *International Journal of Electronics and Electrical Engineering*, Vol. 2, No. 3, September, 2014.
- [3]. Qusay. Salem, Overall Control Strategy of Grid Connected to Wind Farm Using FACTS, *Bonfring International Journal of Power Systems and Integrated Circuits*, Vol. 4, No. 1, February 2014.
- [4]. MojtabaAtabakhsh, Mahmoud Ebadian, MajidrezaNaseh, Transient Stability Enhancement of Wind Farms using Flexible AC Transmission Technology (Comparison of SVC and STATCOM), *International Journal of Innovative Technology and Exploring Engineering*, Vol. 4, Issue. 1, June 2014.
- [5]. C Plumley, W Leithead, P Jamieson, E Bossanyiand M Graham, Comparison of individual pitch and smart rotor control strategies for load reduction, *Journal of Physics: Conference Series* 524 (2014) 012054.
- [6]. Asier González-González , Ismael Etxeberria-Agiriano , EkaitzZulueta , Fernando Oterino-Echavarri and Jose Manuel Lopez-Guede, Pitch Based Wind Turbine Intelligent Speed Setpoint Adjustment Algorithms, *Energies* 2014,7,3793-3809;doi:10.3390/en7063793, www.mdpi.com/journal/energies.
- [7]. N. Dhayanidhi, D.Muralidharan, Dynamic Behavior of DFIG Wind Energy Conversion System under Various Faults, *International Journal of Advanced Research in Electrical, Electronics and Instrumentation Engineering*, Vol. 3, Issue 1, January 2014.
- [8]. Tamilselvan.R, Suganya.P, Rengarajan. N, Control Strategy for DFIG Wind Turbine in Variable Speed Wind Power Generation, *International Journal of Innovative Research in Science, Engineering and Technology*, Vol. 3, Special Issue 1, February 2014.
- [9]. Akash Alex Paret, PID Controlled Frequency Regulation of Wind Turbine, *International Journal of Advanced Research in Electrical, Electronics and Instrumentation Engineering*, Vol. 3, Issue 3, March 2014.
- [10]. Dr.S.K.Purushothaman, DESIGN AND ANALYSIS OF ELIMINATION OF HARMONICS USING WIND ENERGY CONVERSION SYSTEMS, *Journal of Theoretical and Applied Information Technology*, Vol. 61, No.3, March 2014.

- [11]. Akhmatov, V. 2002. Variable-Speed Wind Turbines with Doubly-Fed Induction Generators, *Part I: Modelling in Dynamic Simulation Tools. Wind Engineering Vol. 26, No. 2.*
- [12]. Siano, P. 2007. Design and implementation of a fuzzy controller for wind generators performance optimisation. European Conference on Power Electronics and Applications, *In proc. IEEE Power Electronics and Applications, European Conference, pp. 1-10.*
- [13]. Md. Rafiqul Islam Sheikh, "Stabilization of a Grid Connected Wind Farm by Using SMES" a Ph.D. thesis, September 2010.
- [14]. A.V.A. Macedo and W. S. Mota "Wind turbine pitch angle control using fuzzy logic", *Transmission and Distribution: Latin America Conference and Exposition (T&D-LA), 2012*
- [15]. MATLAB Simulink, version 2012.
- [16]. S. M. Mueeen, J. Tamura, and T. Murata, "Stability Augmentation of a Grid connected Wind Farm," Springer- Verlag, London, ISBN 978-1-84800-315-6, October 2008.
- [17]. M.R.I. Sheikh, S. M. Mueeen, R. Takahashi, Toshiaki Murata and Junji Tamura, "Wind Generator Stabilization by PWM Voltage Source Converter and Chopper Controlled SMES", *Journal of International Review of Automatic Control (I.R.E.A.CO), Vol. 3, pp. 311-320, September 2008.*
- [18]. N. Shenck, "Wind power Systems Wind Energy II", Available online alummi.media.mit.edu/~nate/AES/Wind_Theory_II.pdf.
- [19]. M.R.I. Sheikh, M.A. Matin, M.A. Hossain and M. Shahed "Reference power selection for smoothing wind power fluctuations with reduced energy capacity", *7th International conference on Electrical and Computer Engineering.*
- [20]. PSCADIEMTDC Manual, Manitoba HVDC Research Center (1994).

Md. Shizer Rahman. "Comparison of Different Pitch Controller In Wind Farm For Integrated Power System." American Journal of Engineering Research (AJER), vol. 7, no. 3, 2018, pp. 288-299.